Human Molecular Genetics, 2011, Vol. 20, No. 6 ***1111–1121***
doi:10.1093/hmg/ddq555
Advance Access published on December 24, 2010

Disruption of adaptive energy metabolism and elevated ribosomal p-S6K1 levels contribute to INCL pathogenesis: partial rescue by resveratrol

Hui Wei[1,†], Zhongjian Zhang[1,†], Arjun Saha[1,†], Shiyong Peng[1], Goutam Chandra[1], Zenaide Quezado[2] and Anil B. Mukherjee[1,*]

[1]Section on Developmental Genetics, Program on Developmental Endocrinology and Genetics, Eunice Kennedy Shriver National Institute of Child Health and Human Development and [2]Department of Anesthesia and Surgical Services, NIH Clinical Center, National Institutes of Health, Bethesda, MD 20892-1830, USA

Received August 31, 2010; Revised November 9, 2010; Accepted December 20, 2010

The infantile neuronal ceroid lipofuscinosis (INCL) is a devastating neurodegenerative lysosomal storage disease. Despite our knowledge that palmitoyl-protein thioesterase-1 (PPT1)-deficiency causes INCL, the molecular mechanism(s) of neurodegeneration and the drastically reduced lifespan of these patients remain poorly understood. Consequently, an effective treatment for this disease is currently unavailable. We previously reported that oxidative stress-mediated abnormality in mitochondria activates caspases-9 pathway of apoptosis in INCL fibroblasts and in neurons of *Ppt1*-knockout (*Ppt1*-KO) mice, which mimic INCL. Since mitochondria play critical roles in maintaining cellular energy homeostasis, we hypothesized that oxidative stress-mediated disruption of energy metabolism and homeostasis may contribute to INCL pathogenesis. We report here that, in cultured INCL fibroblasts and in the brain tissues of *Ppt1*-KO mice, the NAD^+/NADH ratio, the levels of phosphorylated-AMPK (p-AMPK), peroxisome proliferator-activated receptor-γ (PPARγ) coactivator-1α (PGC-1α) and Silent Information Regulator T1 (SIRT1) are markedly down-regulated. This suggested an abnormality in AMPK/SIRT1/PGC-1α signaling pathway of energy metabolism. Moreover, we found that, in INCL fibroblasts and in the *Ppt1*-KO mice, phosphorylated-S6K-1 (p-S6K1) levels, which inversely correlate with lifespan, are markedly elevated. Most importantly, resveratrol (RSV), an antioxidant polyphenol, elevated the NAD^+/NADH ratio, levels of ATP, p-AMPK, PGC-1α and SIRT1 while decreasing the level of p-S6K1 in both INCL fibroblasts and in *Ppt1*-KO mice, which showed a modest increase in lifespan. Our results show that disruption of adaptive energy metabolism and increased levels of p-S6K1 are contributing factors in INCL pathogenesis and provide the proof of principle that small molecules such as RSV, which alleviate these abnormalities, may have therapeutic potential.

INTRODUCTION

Neurodegenerative disorders are some of the most intractable human ailments for which the development of effective treatment remains challenging. Neurodegeneration is a devastating manifestation in the majority of more than 40 lysosomal storage disorders that affect 1 in 7000 live-born infants (1,2). Although these storage disorders are rare, they provide a window of opportunity to uncover the pathogenic mechanisms of more common neurodegenerative diseases. Moreover, understanding the molecular mechanism(s) of pathogenesis of these rare disorders may advance our knowledge of the pathogenic mechanism(s) in more common neurodegenerative disorders and facilitate the development of rational therapeutic strategies.

Neuronal ceroid lipofuscinoses (NCLs), also known as Batten disease, represent the most common (1 in 12 500 births) hereditary neurodegenerative storage disorders that primarily affect children (3–8). Mutations in at least eight different genes underlie various types of NCLs. As a group, NCLs

*To whom correspondence should be addressed at: National Institutes of Health, Building 10, Room 9D42, 10, Center Drive, Bethesda, MD 20892-1830, USA. Tel: +1 3014967213; Fax: +1 3014026632; Email: mukherja@exchange.nih.gov
†Equally contributed.

share a number of clinical and pathological features including psychomotor retardation, retinal blindness, myoclonus, seizures, intracellular autofluorescent storage material and reduced lifespan (3–8). The infantile NCL (INCL), also known as infantile Batten disease, is a rare (1 in >100 000 births) but one of the most lethal neurodegenerative storage disorders of childhood caused by inactivating mutations in the palmitoyl protein thioesterase-1 (*Ppt1*) gene (9). Children afflicted with INCL are normal at birth but by 11–18 months of age they develop psychomotor retardation and complete retinal degeneration causing blindness. By age 4, they have no detectable brain activity. These children remain in a vegetative state for another 6–8 years before death (3–8). Despite the fact that the genetic basis of INCL was discovered more than a decade ago (9), the precise molecular mechanism(s) of INCL pathogenesis remains poorly understood and, currently, there is no effective treatment for this disease.

We have previously reported that neurodegeneration in INCL is at least partially caused by excessive endoplasmic reticulum (ER) and oxidative stresses, which mediate neuronal apoptosis (10,11) and neuroinflammation (12,13). We also reported that *Ppt1*-knockout (*Ppt1*-KO) mice (14), which recapitulate virtually all clinical and pathological features of human INCL including dramatically reduced lifespan (15), manifest high levels of oxidative stress, which adversely affects mitochondrial function activating caspase-9 pathway of neuronal apoptosis (11,16). Mitochondria communicate and interact with each other as well as with various cellular organelles such as the ER in order to meet the ever changing cellular energy needs and to protect the cells from excessive Ca^{2+} release as well as mutations in mitochondrial DNA, events that typify aging and neurodegenerative processes (17). Despite varying clinical manifestations of neurodegenerative disorders, the fact that neurons rely heavily on oxidative energy metabolism suggests a unified mechanism that involves dysfunction in mitochondrial energy homeostasis (18).

New insight into the role(s) of mitochondria in neuronal function and viability has been facilitated by the discovery of the peroxisome proliferator-activated receptor-γ (PPARγ) coactivator-1α (PGC-1α), which also regulates thermogenesis (19). Interestingly, we uncovered that thermogenesis in children afflicted with INCL is abnormally regulated (20). In addition to its role in mitochondrial biology, PGC-1α also regulates several key metabolic programs that go beyond mitochondrial biogenesis and oxidative phosphorylation. For example, PGC-1α-null mice manifest defects in adaptive energy metabolism and show clinical manifestations such as stimulus-induced myoclonus, dystonic posturing and frequent limb clasping, characteristic of certain neurodegenerative disorders (21), including INCL.

Impaired mitochondrial energy metabolism due to the disruption of mitochondrial function might negatively affect the ATP/AMP ratio. The cells, especially neurons, in turn respond by adjusting both the anabolic and catabolic pathways of energy metabolism. AMP-activated protein kinase (AMPK) acts as an intracellular energy sensor and plays a pivotal role in maintaining energy balance within the cell (22,23). Emerging evidence indicates that phosphorylation of AMPK (p-AMPK) is critical for maintaining cellular energy reserves by turning on catabolic pathways that generate ATP and biogenesis of mitochondria while switching off anabolic pathways that utilizes ATP (24,25). Moreover, AMPK plays a critical role in mitochondrial biogenesis in response to energy deprivation (26). Recently, it has been reported that AMPK also enhances the activity of SIRT1 (Silent Information Regulator T1), a highly conserved family of NAD^+-dependent deacetylases that regulate lifespan in both lower organisms and in mammals. The roles of mammalian SIRTs have been implicated in resisting cellular stress, tumorigenesis and neurodegeneration (27). AMPK also modulates the activity of down-stream target genes such as PGC-1α, Fork head box O1 (FOXO1) and O3 (FOXO3) transcription factors (28). Further, p-AMPK/SIRT1/PGC-1α signaling pathway plays critical roles in mitochondrial function facilitating adaptive energy metabolism in cells, including the neurons (29).

Resveratrol (RSV) is an antioxidant polyphenol that activates SIRT1 (30,31). It has also been reported that mammalian SIRTs can play critical roles in protecting neurons (32). Moreover, SIRT1 deacetylates a dozen of substrates including PGC-1α and FOXO3a. The most important role played by SIRT1/PGC-1α signaling in neuronal survival has been attested by the fact that transgenic mice in which the expression of PGC-1α is disrupted have neurodegenerative lesions and show behavioral abnormalities (33). Thus, it has been suggested that understanding the AMPK/SIRT1/PGC-1α signaling pathway of energy metabolism, which has not been well documented in the central nervous system, may advance our understanding of the mechanism of neurodegenerative diseases and facilitate the development of novel therapeutic strategies to combat these disorders (34). We hypothesized that oxidative stress may disrupt AMPK/SIRT1/PGC-1α signaling and adversely affect energy homeostasis contributing to INCL pathogenesis. Since oxidative stress is prevalent in virtually all neurodegenerative disorders (17), including INCL, our hypothesis, if correct, may not only be of direct relevance to INCL but also to other more common neurodegenerative disorders.

RESULTS

Altered energy metabolism in the brain of *Ppt1*-KO mice

We hypothesized that oxidative stress-mediated mitochondrial abnormality in PPT1-deficient cells reduce the NAD^+/NADH ratio adversely affecting p-AMPK levels and down-regulate the levels of SIRT1 and PGC-1α, which play important roles in energy metabolism and homeostasis. Accordingly, we determined the levels of p-AMPK in the brain tissues of 1-, 3- and 6-month-old *Ppt1*-KO mice and in those of their WT littermates. The results showed that the levels of p-AMPK in the brains of *Ppt1*-KO mice are progressively down-regulated in an age-dependent manner (Fig. 1A). We then determined p-AMPK levels in normal and INCL fibroblasts. We found that p-AMPK levels are markedly lower in INCL fibroblasts compared with those of their normal counterparts (Fig. 1B). Since AMPK regulates the expression of PGC-1α, we performed western blot analysis of proteins in nuclear fractions of brain tissues from the *Ppt1*-KO mice

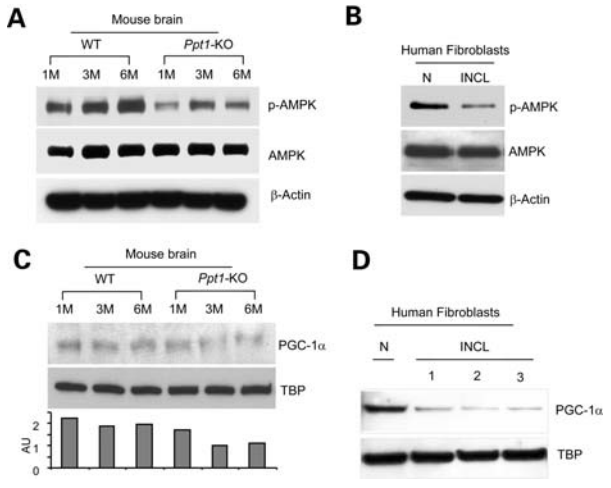

Figure 1. Levels of p-AMPK and PGC-1α in the brain of WT mice, their *Ppt1-KO* littermates and in INCL fibroblasts. (**A**) Western blot analysis of phosphorylated-AMPK (p-AMPK) and total AMPK levels in the brain tissues from 1-, 3- and 6-month WT mice and their *Ppt1*−KO littermates; (**B**) western blot analysis of p-AMPK levels in normal (N, left lane) and INCL patient fibroblasts (right lane); (**C**) western blot analysis of PGC-1α levels in the nuclear fractions of brain tissues from 1-, 3- and 6-month WT mice and their *Ppt1*-KO littermates; (**D**) western blot analysis of PGC-1α in the nuclear fraction from normal human fibroblasts (N) and in that of INCL patient fibroblasts (lanes 1, 2 and 3). TATA box-binding protein (TBP) was used as loading standard for nuclear protein extracts.

and in those of their WT littermates at 1, 3 and 6 months of age. The results showed that PGC-1α levels are markedly decreased in the *Ppt1*-KO mice (Fig. 1C, upper panel). The densitometric analysis of the protein bands further confirmed the results of the western blot (Fig. 1C, lowest panel). We then determined the levels of PGC-1α−protein in nuclear fractions of cultured fibroblasts from a normal and three INCL patients. The results show that compared with the normal fibroblasts, the levels of PGC-1α−protein in those of the INCL patients were significantly lower (Fig. 1D). Taken together, these results suggested that p-AMPK and PGC-1α levels are down-regulated in the brain tissues of *Ppt1*-KO mice as well as in cultured fibroblasts from INCL patients raising the possibility that the regulation of cellular energy metabolism in INCL is abnormally regulated.

Down-regulation of SIRT1 and NAD$^+$/NADH ratio in *Ppt1*-deficient tissues and cells

Since we found lower levels of p-AMPK in *Ppt1*-KO mouse brain tissues, we sought to determine whether lower p-AMPK levels down-regulate the expression of genes involved in energy metabolism in PPT1-deficient cells. We rationalized that this may occur because lower p-AMPK in concert with another metabolic sensor, SIRT1, may disrupt energy metabolism. Accordingly, we tested the level of SIRT1−protein in the nuclear fractions of brain tissues from *Ppt1*-KO mice and in those of their WT littermates. The results of western blot analysis showed that the SIRT1−protein levels in the brain nuclear fractions of *Ppt1*-KO mice are appreciably lower than those of their WT littermates (Fig. 2A). Immunocytochemical analysis of cultured neurons from the *Ppt1*-KO mice and their WT littermates further confirmed these results (Fig. 2B). Consistent with these findings, the SIRT1−protein levels in INCL fibroblasts were also markedly lower compared with those in normal fibroblasts (Fig. 2C). Taken together, these results showed that both in the brain tissues of *Ppt1*-KO mice as well as in INCL fibroblasts SIRT1 levels are significantly lower compared with those of their normal counterparts. Since SIRT1 is activated by an increased NAD$^+$/NADH ratio (28), we sought to determine whether there is a difference in the NAD$^+$/NADH ratio in the brain tissues of *Ppt1*-KO mice and in those of their WT littermates. The results show that the NAD$^+$/NADH ratio in the *Ppt1*-KO mouse brain is significantly lower compared with those of their WT littermates (Fig. 2D). We then determined the NAD$^+$/NADH ratios in cultured normal fibroblasts and in those of their INCL counterparts. The results show a markedly decreased level of NAD$^+$/NADH ratio in INCL fibroblasts (Fig. 2E), suggesting that lower NAD$^+$/NADH ratio in the brain of *Ppt1*-KO mice and in INCL fibroblasts may be one of the reasons for reduced SIRT1 levels. Consistent with these results, the ATP levels in INCL fibroblasts were also considerably lower than those in normal fibroblasts (Fig. 2F).

Amelioration of oxidative stress in *Ppt1-KO* mice and activation of SIRT1 by RSV

We previously reported that the brain tissues in *Ppt1*-KO mice and cultured INCL fibroblasts undergo severe oxidative stress (11,16), which most likely affect the redox state of the cells attested by the reduced NAD$^+$/NADH ratio. To further confirm the presence of oxidative stress, we determined the levels of superoxide dismutase-2 (SOD2) in brain tissues from *Ppt1*-KO mice and in those of their WT littermates. We found significantly elevated SOD2 levels in brain tissues from *Ppt1*-KO mice compared with those of their WT littermates (see Supplementary Material, Fig. S1A).

RSV is a polyphenol with anti-oxidant and SIRT1 activating properties. Since SIRT1 activation is NAD$^+$ dependent (28), we determined whether RSV-treatment improves the NAD$^+$/NADH ratio in INCL fibroblasts. The results showed that RSV treatment improved the NAD$^+$/NADH ratio (Fig. 2G) as well as ATP levels (Fig. 2H) in INCL fibroblasts. These levels declined by 10 h of RSV treatment similar to the decline in NAD$^+$/NADH ratio. We then determined whether SIRT1 levels in INCL fibroblasts are also increased by RSV treatment and as expected, we found that this treatment significantly increased the SIRT1 levels in INCL fibroblasts (Fig. 2I). Taken together, these results suggest that decreased SIRT1 levels in PPT1-deficient cells may be due to a decreased NAD$^+$/NADH ratio and RSV-mediated improvement of NAD$^+$/NADH ratio may increase the SIRT1 levels.

Elevation of phospho-AMPK levels in PPT1-deficient cells by RSV

Since SIRT1 activation leads to the phosphorylation of AMPK, required for its activation, we determined the levels of p-AMPK in untreated and RSV-treated INCL fibroblasts. The results showed that p-AMPK levels in RSV-treated

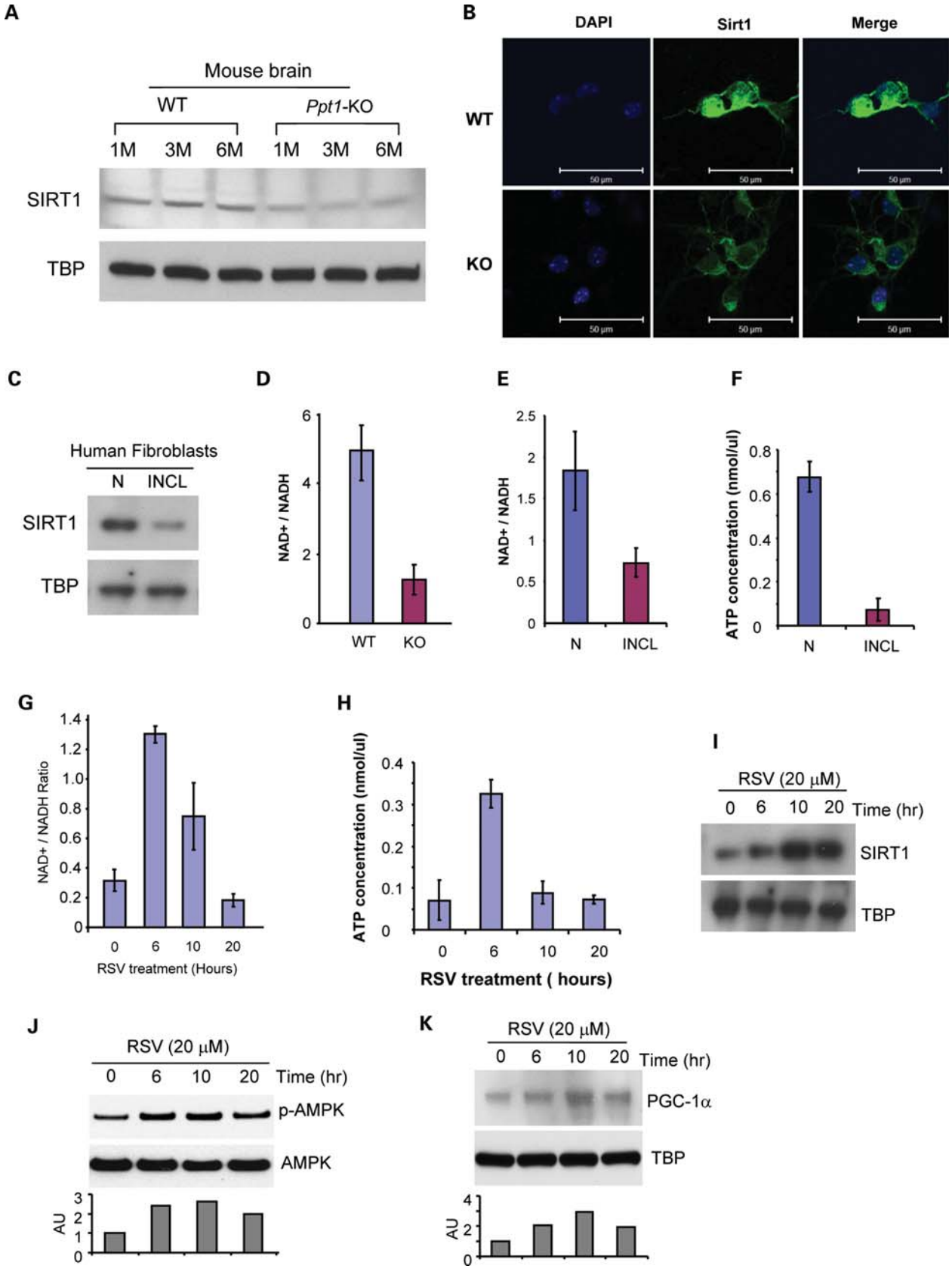
A
Mouse brain
WT
Ppt1-KO
1M 3M 6M 1M 3M 6M
SIRT1
TBP
B
DAPI
Sirt1
Merge
WT
KO
50 µm
C
Human Fibroblasts
N INCL
SIRT1
TBP
D
NAD+ / NADH
WT KO
E
NAD+ / NADH
N INCL
F
ATP concentration (nmol/ul)
N INCL
G
NAD+ / NADH Ratio
0 6 10 20
RSV treatment (Hours)
H
ATP concentration (nmol/ul)
0 6 10 20
RSV treatment (hours)
I
RSV (20 µM)
0 6 10 20 Time (hr)
SIRT1
TBP
J
RSV (20 µM)
0 6 10 20 Time (hr)
p-AMPK
AMPK
AU
K
RSV (20 µM)
0 6 10 20 Time (hr)
PGC-1α
TBP
AU

INCL fibroblasts are appreciably elevated (Fig. 2J). The densitometric analysis of the protein bands further confirmed the western blot results (Fig. 2J, lowest panel). We then sought to determine whether RSV also stimulates PGC-1α levels in INCL fibroblasts. The data showed that RSV treatment of INCL fibroblasts also increased the PGC-1α levels in a time-dependent manner (Fig. 2K). These results are further confirmed by densitometric analysis of the protein bands (Fig. 2K, lowest panel). AICAR (5-Aminoimidazole-4-carboxyamide ribonucleoside), an adenosine analog which is taken up by cells generating its phosphorylated form, 5-aminoimidazole-4-carboxamide-1-D-ribofuranosyl-5′-monophosphate, stimulates AMPK activity (35). We sought to determine whether AICAR, like RSV, also stimulates p-AMPK and PGC-1α levels in INCL fibroblasts. Accordingly, we treated INCL fibroblasts with AICAR and determined the levels of p-AMPK and PGC-1α. We found that AICAR-treatment of the INCL fibroblasts markedly elevated the levels of p-AMPK and PGC-1α in a time-dependent manner (see Supplementary Material, Fig. S1B). Taken together, these results suggest that RSV treatment increases the NAD^+ /NADH ratio and the levels of SIRT1, p-AMPK as well as PGC-1α, which is likely to improve cellular energy metabolism in *Ppt1*-KO mouse brain, cultured neurons from *Ppt1*-KO mice and in cultured INCL fibroblasts.

RSV diet increases the levels of p-AMPK, SIRT1 and PGC-1α in *Ppt1*-KO mouse brain

Since the results of our *in vitro* experiments indicate that RSV treatment increases the levels of SIRT1, NAD^+/NADH ratio, p-AMPK and PGC-1α, which are critical for regulating energy metabolism, we sought to validate these observations *in vivo*. Accordingly, we carried out experiments in which *Ppt1*-KO mice were fed either normal diet (control) or a diet, which consisted of normal diet containing RSV. The mice were fed these diets for 2 months starting at 4 months of age. We chose to use 4-month-old mice, as they manifest virtually no symptoms of INCL, whereas at 6-months of age these mice show signs of neurological impairment. We used a dose of RSV (0.2 g/100 g mouse chow) that is equivalent to 600 mg RSV/day/kg body weight (see Materials and Methods section). This dose of RSV has been reported to be safe and produce no adverse effects (36). The results showed that compared with untreated *Ppt1*-KO mice those on RSV diet had significantly elevated level of p-AMPK (Fig. 3A), SIRT1 (Fig. 3B) as well as PGC-1α (Fig. 3C).

Previous *in vitro* experiments have shown that SIRT1 stimulates the expression and activation of its downstream FOXO transcription factors in various cell types as these transcription factors regulate cellular capacity to cope with ER and oxidative stresses (37,38). Therefore, we first determined the levels of FOXO3a protein in the brain tissues of *Ppt1*-KO mice and in those of their WT littermates. The results showed that compared with the WT littermates the baseline levels of FOXO3a protein in the brain of *Ppt1*-KO mice were markedly lower (see Supplementary Material, Fig. S1C). We then determined the FOXO3a levels in the brain tissues of RSV-fed *Ppt1*-KO mice. Most notably, feeding RSV-diet for 2 months to the *Ppt1*-KO mice stimulated the FOXO3a levels (see Supplementary Material, Fig. S1D). These results demonstrated that feeding of RSV-containing diet may improve AMPK/SIRT1/PGC-1α signaling pathway in *Ppt1*-KO mice and augment energy homeostasis *in vivo*.

RSV stimulates mitochondrial biogenesis in *Ppt1*-deficient cells

Current evidence indicates that SIRT1 not only activates PGC-1α but also promotes mitochondrial biogenesis, and RSV simulates PGC-1α activity improving mitochondrial function (39). Most recently, it has been shown that activation of PGC-1α also regulates mitochondrial density in neurons (40). Since we found that SIRT1 and PGC-1α levels in *Ppt1*-KO mouse brain as well as in INCL fibroblasts is markedly down-regulated, we sought to determine whether the low levels of SIRT1 and PGC-1α also correlate with lower mitochondrial density. Accordingly, we used Mitotracker fluorescence to measure mitochondrial density in cultured primary neurons from WT mice and in those of their *Ppt1*-KO littermates. Our results showed that compared with the neurons from WT mice (Fig. 3D) those from the *Ppt1*-KO littermates showed markedly lower level of mitochondrial density (Fig. 3E). We then treated the cultured neurons from *Ppt1*-KO mice with RSV (20 μM) and found that RSV treatment significantly increased the levels of mitochondrial density (Fig. 3F). Quantitation of Mitotracker fluorescence by densitometry further confirmed these results (Fig. 3G), indicating that RSV is capable of stimulating mitochondrial biogenesis and density in cultured neurons from *Ppt1*-KO mice.

Mitochondrial biogenesis, adaptive thermogenesis, respiration, insulin secretion and gluconeogenesis are also regulated by PGC-1α (19). The biogenesis and maintenance of mitochondrial function are regulated by several transcription factors, including mitofusin (Mfn), fission 1 (Fis1) and mitochondrial factor A (TFAM) (41). Since we found that in *Ppt1*-KO mice oxidative stress disrupts energy metabolism as attested by lower levels of p-AMPK, SIRT1 and PGC-1α, we determined Mfn1-, Fis1- and TFAM-mRNA levels in

Figure 2. Effects of RSV on levels of SIRT1, p-AMPK, PGC-1α, NAD^+/NADH ratio and ATP levels. (**A**) Western blot analysis of SIRT1 in nuclear fractions prepared from the cerebral cortex of 1-, 3- and 6-month-old WT mice and their *Ppt1-KO* littermates using Rabbit anti-SIRT-1 antibody. TATA box-binding protein (TBP) was used as loading standard for nuclear protein extracts; (**B**) immunocytochemical analysis of SIRT-1 (green) in cultured neurons derived from WT mice (upper panels) and their *Ppt1-KO* littermates (lower panels). DAPI (blue) was used to stain the nucleus; (**C**) western blot analysis of SIRT1 in nuclear fractions of normal human fibroblasts and INCL patient fibroblasts; (**D**) NAD^+/NADH ratios in brain tissues of 6-month-old WT mice and their *Ppt1-KO* littermates; (**E**) NAD^+/NADH ratios in normal and INCL fibroblasts; (**F**) ATP levels in normal and INCL fibroblasts; (**G**) NAD^+/NADH ratios in INCL fibroblasts treated with 20 μM RSV; (H) ATP levels in INCL fibroblasts treated with 20 μM RSV for 6–20 h; (**I**) western blot analysis of SIRT1– protein in untreated and RSV-treated INCL fibroblasts; (**J**) western blot analysis of p-AMPK levels in untreated and RSV-treated INCL fibroblasts. Bar graphs represent densitometric quantitation of the protein bands ± SD ($n = 3$ independent experiments); (**K**) western blot analysis of PGC-1α protein levels in untreated and RSV-treated INCL fibroblasts. Bar graphs represent densitometric quantitation of the protein bands.

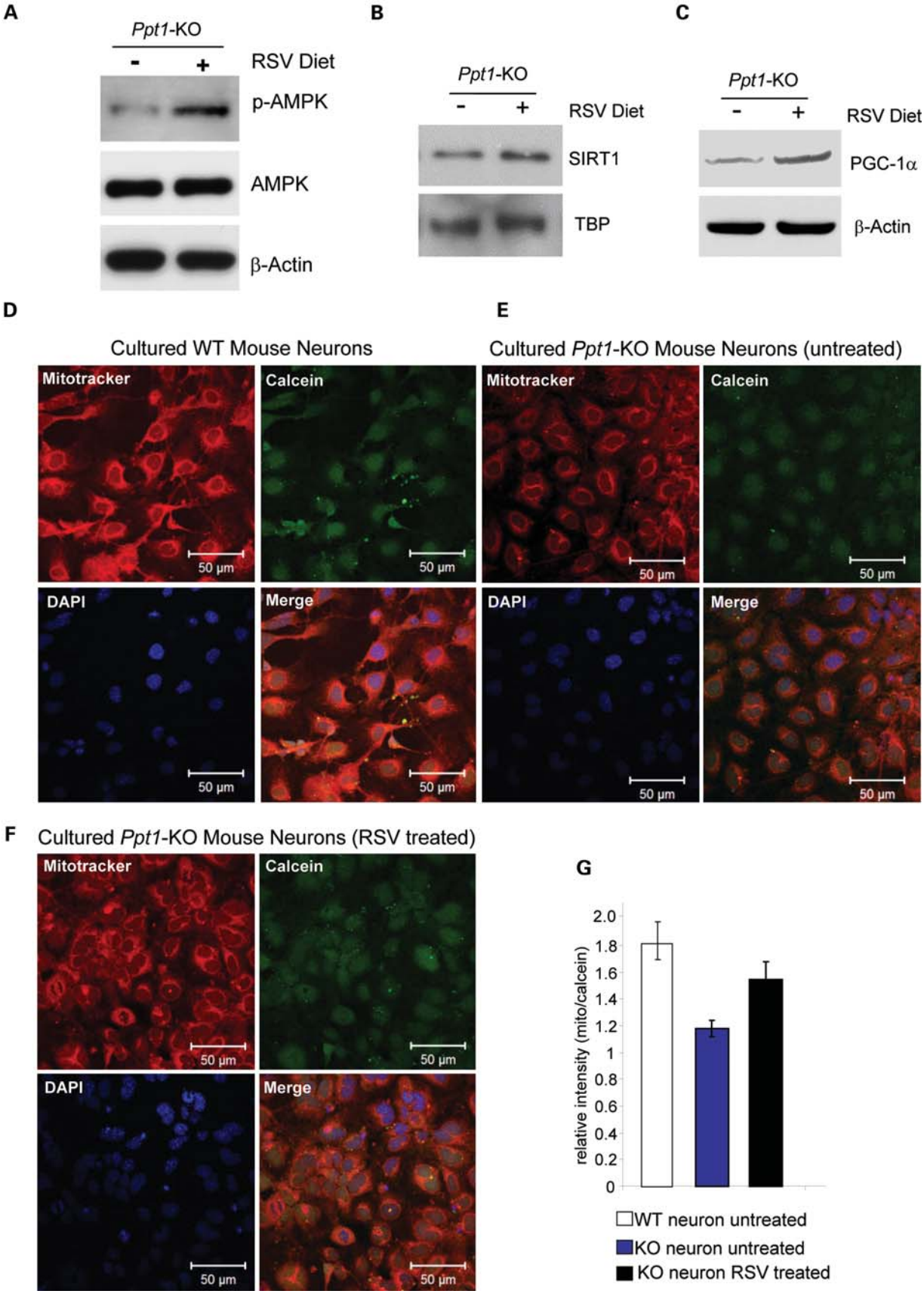
A
Ppt1-KO
- +
RSV Diet
p-AMPK
AMPK
β-Actin
B
Ppt1-KO
- +
RSV Diet
SIRT1
TBP
C
Ppt1-KO
- +
RSV Diet
PGC-1α
β-Actin
D
Cultured WT Mouse Neurons
Mitotracker
Calcein
DAPI
Merge
50 μm
E
Cultured Ppt1-KO Mouse Neurons (untreated)
Mitotracker
Calcein
DAPI
Merge
50 μm
F
Cultured Ppt1-KO Mouse Neurons (RSV treated)
Mitotracker
Calcein
DAPI
Merge
50 μm
G
relative intensity (mito/calcein)
2.0
1.8
1.6
1.4
1.2
1
0.8
0.6
0.4
0.2
0
WT neuron untreated
KO neuron untreated
KO neuron RSV treated

normal and INCL fibroblasts. The results showed that the mRNA levels of all three transcription factors are markedly down-regulated in INCL fibroblasts compared with those in normal fibroblasts (see Supplementary Material, Fig. S2A). We then determined the mRNA levels of Mfn1, Fis1 and TFAM in normal as well as untreated- and RSV-treated INCL fibroblasts. The results showed that RSV stimulated the mRNA levels of all three transcription factors in a time-dependent manner (see Supplementary Material, Fig. S2B). To determine whether these results are reproducible *in vivo*, we determined the mRNA levels of Mfn, Fis1 and TFAM in normal and *Ppt1*-KO mice that were on normal diet as well as those that were on RSV diet. Our results showed that RSV diet stimulated the mRNA levels of all three transcription factors in PPT1-deficient cells (see Supplementary Material, Fig. S2C). Taken together, these results strongly suggested that RSV stimulates the genes critical for mitochondrial biogenesis both *in vitro* and *in vivo*.

Suppression of neuronal apoptosis and inhibition of astroglial activation by RSV in *Ppt1*-KO mice

We previously reported that neuronal degeneration in INCL is at least partially mediated by increased apoptosis due to increased ER and oxidative stresses (11,16,17,35). Since RSV has anti-oxidative properties (40), we hypothesized that it may have beneficial effects on PPT1-deficient cells. In addition, RSV is an activator of SIRT1 as well as PGC-1α and it crosses the blood brain barrier (30). Thus, we sought to determine whether this compound has anti-apoptotic effects in the brain of the *Ppt1*-KO mice. Accordingly, we performed western blot analyses of brain tissues of WT mice and their *Ppt1*-KO littermates either on control- or RSV-diet and determined the levels of cleaved PARP-1 (marker for apoptosis), synaptophysin (marker for neurons) and glial fibrillary acidic protein (GFAP), which is a marker for activated astroglial cells. The results showed that compared with the WT littermates the brain tissues of *Ppt1*-KO mice on control diet showed significantly higher level of cleaved PARP-1 (Fig. 4A, top panel), lower level of synaptophysin (Fig. 4A, second panel) and higher level of GFAP (Fig. 4A, third panel). The β-actin levels, used as protein-loading standard, were virtually identical (Fig. 4A, bottom panel). These results indicated that in the brain of *Ppt1*-KO mice there was more apoptosis, less neuronal cells and increased astroglial activation, which occur in most neurodegenerative disorders, including INCL. Most importantly, *Ppt1*-KO mice on RSV diet showed an appreciably lower level of cleaved PARP-1 (Fig. 4A, top panel), higher level of synaptophysin (Fig. 4A, second panel) and lower level of GFAP (Fig. 4A, third panel). Taken together, these results strongly suggest that RSV not only improves cellular energy metabolism but also protects neurons from apoptosis.

RSV diet modestly improves longevity in *Ppt1*-KO mice

In several model organisms, RSV has been reported to stimulate SIRT1/PGC-1α signaling pathways to expand lifespan (28). Recently, it has also been demonstrated that a 15–20% increase in lifespan may be achieved in obese mice fed with a diet containing RSV (41). However, more recently, it has been reported that, in normal aging mice, RSV may delay age-related deterioration of functions but may not increase lifespan (42). Since in our experiments RSV appeared to improve several parameters that are known to improve neuronal function, we sought to determine whether RSV diet may also improve longevity in *Ppt1*-KO mice. Accordingly, we fed *Ppt1*-KO mice with a diet containing RSV and compared their longevity with that of their littermates that were fed with the same diet but without RSV. Our results showed that *Ppt1*-KO mice that were on RSV diet for 4 months had a small increase in lifespan (36.7 ± 0.6 weeks) (Fig. 4B, dotted line) compared with the control *Ppt1*-KO mice that received no RSV in their diet (34.6 ± 0.7 weeks) (Fig. 4B, solid line). These results indicate that feeding of RSV diet to *Ppt*1-KO mice not only protects against neurodegeneration but may also cause a small increment in their lifespan.

Recently, it has been reported that phosphorylated-p70 ribosomal protein S6 kinase-1 (p-S6K1) levels inversely correlate with lifespan in mice (43). The lifespan of the *Ppt1*-KO mice is curtailed significantly as they die ∼8 months of age (normal lifespan 24 months). Therefore, we determined the levels of p-S6K1 in brain tissues of *Ppt1*-KO mice. The results showed that *Ppt1*-KO mice have significantly elevated levels of p-S6K1 (Fig. 4C), which is consistent with the prediction of decreased lifespan (43). Moreover, we also found that the levels of PI3K and Akt, which up-regulate mTOR activity by its ability to phosphorylate S6K1, are also markedly elevated in the *Ppt1*-KO mice (see Supplementary Material, Fig. S3A and B). This may explain why the levels of p-S6K1 in the *Ppt1*-KO mice are significantly elevated. Interestingly, *Ppt1*-KO mice on RSV diet showed markedly reduced levels of p-Akt and PI3K (see Supplementary Material, Fig. S3C). Most importantly, *Ppt1*-KO mice on RSV diet also showed markedly reduced level of p-S6K1 (Fig. 4D). Taken together, results suggest that RSV may at least in part mediate the increased lifespan in the *Ppt1*-KO mice by down-regulating the p-S6K1 levels.

Figure 3. RSVstimulates brain p-AMPK, SIRT1, PGC-1α levels and mitochondrial density in cultured neurons from *Ppt1*-KO mice. (**A**) Western blot analysis of p-AMPK levels in the brain tissues of untreated and RSV-treated *Ppt1*-KO mice. (**B**) Western blot analysis of SIRT1–protein levels in the brain tissues of untreated- and RSV-treated *Ppt1*-KO mice. (**C**) Western blot analysis of PGC-1α protein levels in the brain tissues of untreated and RSV-treated *Ppt1*-KO mice. Mitotracker staining (red) showing mitochondrial densities in cultured neurons: (**D**) neurons from WT mice; (**E**) neurons from *Ppt1*-KO without RSV treatment and (**F**) neurons from *Ppt1*-KO mice were treated with 20 μM RSV for 20 h. Calcein (green) dye was used to stain the cytoplasm and DAPI (blue) to localize the nuclei. (**G**) Densitometric analyses of relative intensities of Mitotracker/calcein ratio in cultured neurons from WT and *Ppt1*-KO mice. Mitochondrial density was quantified by calculating the ratio of average fluorescence intensity of Mitotracker (red, representing the mitochondria) versus Calcein (green, representing the entire cytoplasm of a cell) using LSM image analysis software (Carl Zeiss). Statistical analysis of the results was performed using Student's *t*-test. Each experiment was repeated at least six times. Compared with WT neurons untreated *Ppt1*-KO neurons showed a significantly reduced fluorescence ($P < 0.0001$; $n = 6$ independent experiments). We then compared the fluorescence levels in untreated and RSV-treated *Ppt1*-KO neurons. The results showed a significant increase in fluorescence in the RSV-treated Ppt1-KO neurons ($P < 0.0008$; $n = 6$ independent experiments). WT (open bar); RSV-untreated *Ppt1*-KO neurons (blue bar) and RSV-treated *Ppt1*-KO neurons (black bar).

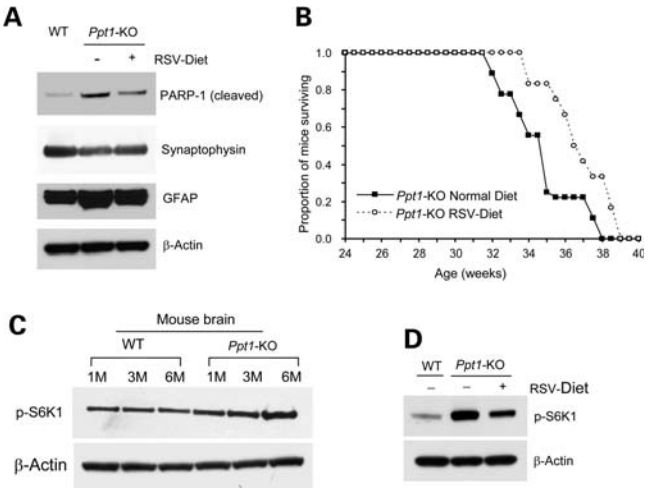

Figure 4. RSVsuppresses apoptosis, reduces p-S6K1 level and expands lifespan in *Ppt1*-KO mice. (**A**) Western blot analysis of apoptotic cell-marker, cleaved-Parp-1 (top panel), neuronal marker, synatophysin (second panel) and astroglial marker, GFAP (third panel) in the brain lysates of WT mice and their *Ppt1*-KO littermates on normal diet, or on RSV diet. β-Actin (bottom panel) was used as protein-loading standard. (**B**) Lifespan of *Ppt1*-KO mice fed a normal- (solid line) or RSV-containing diet (dotted line). Mice were fed either normal diet ($n = 10$) or normal diet containing RSV ($n = 12$). The average lifespan for the mice on normal diet (solid line) is compared with that of the mice fed the RSV diet (dotted line). The calculated lifespan of *Ppt1*-KO mice on normal diet was 34.6 ± 0.7 and of those on RSV diet was 36.7 ± 0.6 weeks, respectively. (**C**) Western blot analysis of phosphorylated-S6K1 levels in the brain tissues from 1-, 3- and 6-month-old WT mice and their *Ppt1*-KO littermates; (**D**) western blot analysis of phosphorylated-S6K1 in the brain tissue lysates of WT mice and their *Ppt1*-KO littermates on normal diet, or on RSV diet.

DISCUSSION

In this study, we demonstrated that, in cultured cells from INCL patients as well as in the brain of *Ppt1*-KO mice, the levels of p-AMPK, SIRT1 and PGC-1α, which play critical roles in cellular energy metabolism and homeostasis, are markedly down-regulated. In addition, we showed that in *Ppt1*-KO mice p-S6K1 level, which inversely correlates with lifespan, is significantly elevated. Most importantly, RSV, an anti-oxidant polyphenol that activates SIRT1, reversed these abnormalities in both cultured INCL cells and in the brain tissues of *Ppt1*-KO mice, which showed a small increase in lifespan.

INCL is a lysosomal storage disease caused by inactivating mutations in the *PPT1* gene (9). Lysosomal enzyme deficiency impairs degradative and metabolic processes causing abnormal accumulation of partially degraded substrates. It has been suggested that because of this abnormality in lysosomes the undegraded material may be considered an energy storage depot, which remains inaccessible to the cell; however, the maintenance of the storage depot requires energy, thereby contributing negatively to energy balance (44). Our results showed that the levels of p-AMPK, SIRT1 and PGC-1α, which are critical for regulating energy metabolism and homeostasis, is clearly abnormal in cultured INCL fibroblasts and in the brain of *Ppt1*-KO mice. Moreover, the fact that these abnormalities were reversed by RSV treatment suggests that abnormal energy metabolism is a contributing factor in INCL pathogenesis.

How might RSV increase the longevity in the *Ppt1*-KO mice? Genetic studies in yeast and *Drosophila* have implicated several mechanisms that control lifespan (45). Among these are insulin and insulin-like growth factor 1 (IGF-1) signaling as well as the mammalian target of rapamycin (mTOR) pathways. IGF-1 signaling and mTOR pathways activate the downstream effector, P70 ribosomal S6 protein kinase-1 (S6K1) and, recently, it has been reported that phosphorylated S6K1 (p-S6K1) levels inversely correlate with lifespan in mice (43). The lifespan of the *Ppt1*-KO mice is curtailed significantly as they die ∼8 months of age. Our results showed that *Ppt1*-KO mice have significantly elevated levels of p-S6K1, which is consistent with the prediction that these mice may have decreased lifespan. Moreover, our results also showed increased levels of PI3K and Akt that may up-regulate mTOR activity, which in turn phosphorylates S6K1. This may explain our finding that the levels of p-S6K1 in the *Ppt1*-KO mice are significantly elevated. Remarkably, *Ppt1*-KO mice on RSV diet showed markedly reduced levels of p-Akt and PI3K and, most importantly, *Ppt1*-KO mice on RSV diet also showed a significantly reduced level of p-S6K1. Taken together, our results suggest that RSV may have caused a small increase in lifespan in *Ppt1*-KO mice at least in part due to the down-regulation of p-S6K1 levels. RSV has been reported to prolong lifespan and retard age-related deterioration in short-lived vertebrates (46). Recently, it has been reported that, although RSV mimics transcriptional aspects of caloric restriction and delays age-related deterioration, it does not increase lifespan in normal aging mice (42). The discrepancy between these findings and those of our present study may be due to the fact that *Ppt1*-KO mice have a very limited lifespan (8 versus 24 months in normal mice) and while RSV modestly increased this short lifespan of these mice, it may not have had a significant effect on prolonging the total lifespan of normal aging mice as previously reported (42). The results of our present study show that RSV increases SIRT1-mRNA and SIRT1-protein levels but we have not measured SIRT1 enzymatic activity. It is important to note that currently, a mechanism(s) by which RSV mimics the effects of caloric restriction and expands lifespan remains unclear. On the basis of our present findings, we provide a model (Fig. 5) to explain a likely mechanism by which RSV may improve energy metabolism and homeostasis that in turn cause a small increase in lifespan of the *Ppt1*-KO mice. It should be noted that our estimate of lifespan increase was determined when *Ppt1*-KO mice were still active enough to reach for food and water. They were euthanized before they went into vegetative state for humanitarian reason. A small increase in lifespan observed in RSV-treated animals is not the ultimate goal of our present study. Nonetheless, it provides a framework in which more potent small molecules that reduce oxidative stress, up-regulate the levels of p-AMPK, SIRT1 and PGC-1α and decrease the p-S6K1 level may be tested for their therapeutic potential for INCL and possibly for other neurodegenerative disorders.

MATERIALS AND METHODS

Cell lines and chemicals

The normal human fibroblasts (GM00497 and GM00969) were obtained from Coriell Institute for Medical Research,

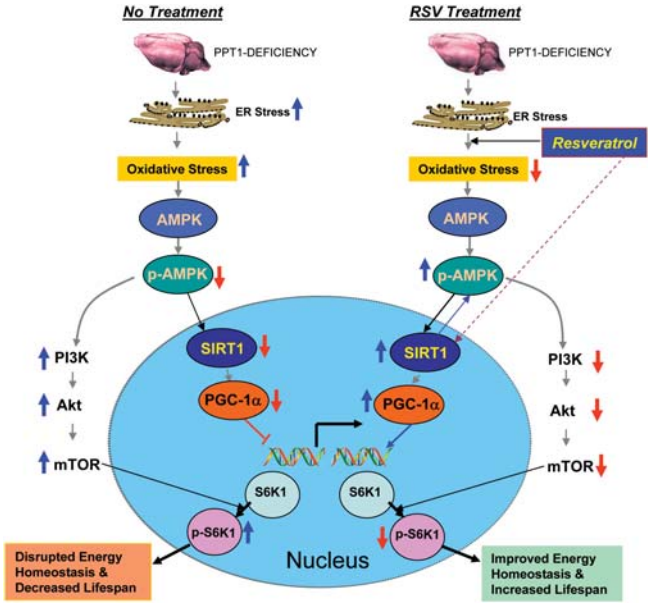

Figure 5. A model explaining how RSV may mediate energy homeostasis and lifespan expansion in *Ppt1*-KO mice. Increased ER and oxidative stresses lead to neuronal apoptosis (left upper). Oxidative stress reduces the levels of p-AMPK (phosphorylated-AMPK) most likely by inhibiting the protein kinase, LKB1 that is known to phosphorylate AMPK. Down-regulation of p-AMPK reduces the level and activation of SIRT1, which in turn reduces PGC-1α. As a result, expression of genes down-stream from PGC-1α is down-regulated disrupting energy homeostasis. Down-regulation of p-AMPK levels also stimulates PI3K (phosphatidylinositol 3-kinase), which in turn activates Akt. The activation of Akt leads to the phosphorylation and activation of mTOR (mammalian target of rapamycin) that is known to phosphorylate S6K1 (ribosomal S6 protein kinase 1). Increased p-S6K1 levels inversely correlates with lifespan (43). RSV, an SIRT1-activator and an antioxidant polyphenol, not only reduces oxidative stress but also increases p-AMPK levels most likely by stimulating LKB1. Thus, RSV stimulates the PGC-1α level that increases the expression of genes down-stream of PGC-1α. Activated SIRT1 may also enhance p-AMPK levels. By increasing the p-AMPK levels, RSV also suppresses activation of PI3K/Akt pathway of mTOR activation, which decreases the p-S6K1 levels, thereby increasing lifespan. Therefore, by stimulating p-AMPK/SIRT1/PGC-1α signaling pathway and suppressing p-S6K1 levels, RSV improves energy homeostasis in neurons and in other cell types in the *Ppt1*-KO mice and causes a small increase in lifespan. As suggested by the results obtained from INCL fibroblasts, RSV may have similar beneficial effects on INCL patients.

and two PPT1-deficient fibroblast lines were derived from IBD patients. The fibroblasts were cultured in DMEM supplemented with 10% heat-inactivated fetal bovine serum (FBS), 2 mM glutamine, 100 U/ml penicillin and streptomycin. Cells were maintained at 37°C in a humidified 5% CO_2 atmosphere. Neurons were isolated from E15 embryonic brain cortex of WT and *Ppt1*-KO mice and cultured and maintained in Neurobasal medium supplemented with B27 (Invitrogen, Carlsbad, CA, USA).

RSV treatment of cultured cells

RSV used in the human fibroblast treatment was purchased from Sigma R5010. Fibroblasts were plated with a density of 1×10^4 cells per cm^2 and 24 h after seeding; they were fed a medium containing RSV. An appropriate volume of RSV stock solution (0.25 M in DMSO was added to the cell culture medium to obtain the final concentrations of RSV (20 μM). For determining the time course, cells were cultured in a medium containing a fixed concentration (20 μM) of RSV in DMSO. The final concentration of DMSO in the medium was 0.02%. The cells were cultured in RSV or DMSO medium for 0, 3, 6, 10, 20, 36, 48 h. For the dose–response treatment, a fixed treatment time of 10 h was used, the concentration of RSV was 0, 5, 20, 300 μM, and the final vehicle (DMSO) concentration in the medium was all adjusted to 0.12% to exclude the potential influence that this level of DMSO may have on the investigated parameters. In both time– and dose–response treatments, a parallel experiment exposing the cells to 0.12% DMSO was set as a control to calibrate the observed results (data not shown).

Animals and diets

The *Ppt1*-KO mice were generated in the laboratory of Dr Sandra Hofmann (14). The mice were extensively backcrossed to obtain a homogenous C57 genetic background in the laboratory of Dr Mark Sands and a mating pair was obtained from his laboratory. All animal experiments were performed according to a protocol approved by the institutional Animal Care and Use Committee. The mice were fed standard NIH-31 diet (Zeigler Brothers, Gardner, PA, USA) as the normal diet, or with RSV-diet, which is the standard NIH-31 diet containing RSV as prepared as described below. The animals were housed three per cage in standard cages and under a light cycle of 12 h light–dark. They had *ad libitum* access to drinking water and the normal diet or RSV diet throughout the experiment.

Preparation of RSV diet

RSV (mol. wt. 228) was purchased from Orchid (Chennai, India). The previously reported doses of RSV in the diet were 0.04–0.4 g/100 g of mouse chow (41). In the present study, we used 0.2 g RSV per 100 g chow, which provides a dose of 600 mg RSV/day/kg body weight. This calculation is based on 6 g of chow consumption per day per mouse as reported previously (41), assuming an average body weight of a mouse to be 20 g. Appropriate amounts of normal diet and RSV diet were prepared daily according to the total number of mice used in our experiment. Four milliliters of 100% ethanol (for normal control diet) or RSV stock solution (for RSV diet) were sprayed onto 100 g of pulverized chow and thoroughly mixed. RSV stock solution at a concentration of 50 mg RSV/ml of ethanol was kept at −80°C. The ethanol in the freshly prepared diet was evaporated overnight in the dark at room temperature. Food cups along with the remaining diet were replaced with freshly prepared diet each morning. Food cups were covered with galvanized wire mesh (1.3 cm) that allowed access of 'head-only', a measure that minimizes the wastage of pulverized diet. The uneaten food was replaced with freshly prepared diet every morning.

Longevity studies using untreated and RSV diet-consuming *Ppt1*-KO mice

Longevity studies were conducted similar to RSV treatment except that the mice were put on RSV diet and maintained

on this diet. When the mice were too feeble to reach the food cups or the drinking bottle, their age data were recorded and the mice were sacrificed.

NAD^+/NADH and ATP assays

Twenty milligrams of freshly isolated brain cortical tissues from WT mice and their *Ppt1*-KO littermates were homogenized, and total NAD^+ and NADH levels were determined according to the protocol provided in the NAD^+/NADH Assay Kit (Abcam, Inc., Cambridge, MA, USA). NAD^+/NADH ratios in WT mice ($n = 3$) and in their *Ppt1*-KO littermates ($n = 3$) were plotted. ATP levels in normal control fibroblasts as well as those in untreated and RSV-treated INCL fibroblasts were measured using a fluorometric assay kit (BioVision Research Products) according to supplier's instructions. ATP concentration in each sample was calculated from a standard curve.

Real-time RT–PCR

Real-time RT–PCR reactions were performed as reported previously (10,16). These reactions were performed in triplicate and repeated in at least two independent experiments. The sequences of primers for the real-time RT–PCR are listed in Supplementary Material, Table S1.

Western blot analysis

Cell lysates or mice cerebral cortex lysates were prepared using PhosphoSafe extraction reagent (EMD Biosciences). Western blot analyses were performed according to the procedure described previously (10,16). The primary antibodies used in the present study are anti-β-actin (1:2000; US Biological), anti-p-AMPK (1:1000, Cell Signaling Tech.), anti-AMPK(1:1000, Cell Signaling Tech.), anti-p-S6K (1:1000, Cell Signaling Tech.), anti-cleaved PARP (Asp214) (1:1000, BD Pharmingen.), anti-p-AKT(ser 473) (1:1000, Cell Signaling Tech.), anti-p-AKT(Thr 308) (1:1000, Cell Signaling Tech.), anti-AKT (1:1000, Cell Signaling Tech.), anti-PI3K (1:2000; Epitomics), anti-SOD2 (1:1000; Santa Cruz), anti-FOXO3A (1:1000; Upstate), anti-GFAP (1:1000, Affinity Bioreagents), anti-PGC-1α (1:500; Santa Cruz or Chemicon) and anti-SIRT1 (1:2000, clone 2G1/F7, Upstate), anti-synaptophysin (1:7500, Abcam), anti-TFIID (TBP) (1:250; Santa Cruz). The sources for the secondary antibodies are as described previously (10).

Confocal microscopy

The WT and *Ppt1*-KO primary neurons were incubated at 37°C in an atmosphere of 5% of CO_2 and 95% air for 24 h. Cells were washed three times with PBS, pH 7.6, and incubated in 4.0% formaldehyde solution for 15 min for fixation. The fixed cells were incubated with antibodies to Sirt1 (1:50), incubated overnight at 4°C in PBS, pH 7.6, containing 2% BSA. Goat anti-rabbit-alexafluor488-conjugated secondary antibody (Invitrogen) was used in PBS, pH 7.6, containing 2% BSA at room temperature for 1 h. Nuclei were stained with 4,6-diamidino-2-phenylindole dihydrochloride (DAPI, Sigma). After three washes with PBS, fluorescence was visualized using an LSM-510 inverted confocal microscope (Zeiss), and the images were processed with the LSM Image Browser, version 4.2 (Zeiss).

Determination of mitochondrial density

We used Mitotracker Red CMXRos (Molecular probes) and Calcein AM (Calbiochem) for labeling neuronal mitochondria and cytosol, respectively, as per manufacturer's instructions. Briefly, five to six DIV (days *in vitro*)-cultured neurons ($1–2 \times 10^5$ cells/well) from WT or *Ppt1*-KO neonates previously treated with RSV or vehicle were washed in serum-free medium and incubated in pre-warmed (37°C) staining solution containing 100 nM Mitotracker Red and 1 μM Calcein AM for 45 min in a 37°C CO_2 incubator. After the staining, the cells were washed in PBS, fixed, counterstained with DAPI and observed under a confocal fluorescence microscope.

SUPPLEMENTARY MATERIAL

Supplementary Material is available at *HMG* online.

ACKNOWLEDGEMENTS

We thank Dr Sandra L. Hofmann for the generous gift of the *Ppt1*-KO mice generated in her laboratory (14). We also thank Drs S.W. Levin, J.Y. Chou and I. Owens for critical review of the manuscript and helpful suggestions. We are grateful to V. Schram [Microscopy and Imaging Core, *Eunice Kennedy-Shriver* National Institute of Child Health and Human Development (NICHD)] for his help with confocal microscopy.

FUNDING

This research was supported in part by the Intramural Research Program of the Eunice Kennedy Shriver National Institute of Child Health and Human Development, National Institutes of Health and the Batten Disease Support and Research Association (BDSRA).

REFERENCES

1. Sly, W.S. and Vogler, C. (2002) Brain-directed gene therapy for lysosomal storage disease: going well beyond the blood-brain-barrier. *Proc. Natl Acad. Sci. USA*, **99**, 5760–5962.
2. Proia, R.L. and Wu, Y.P. (2004) Blood to brain to the rescue. *J. Clin. Invest.*, **113**, 1108–1110.
3. Cooper, J.D., Russell, C. and Mitchison, H.M. (2006) Progress towards understanding disease mechanisms in small vertebrate models of neuronal ceroid lipofuscinosis. *Biochim. Biophys. Acta*, **1762**, 873–889.
4. Haltia, M. (2006) The neuronal ceroid-lipofuscinoses: from past to present. *Biochim. Biophys. Acta*, **1762**, 850–856.
5. Jalanko, A., Tyynelä, J. and Peltonen, L. (2006) From genes to systems: new global strategies for the characterization of NCL biology. *Biochim. Biophys. Acta*, **1762**, 934–944.
6. Goebel, H.H. and Wisniewski, K.E. (2004) Current state of clinical and morphological features in human NCL. *Brain Pathol.*, **14**, 61–69.
7. Mitchison, H.M. and Mole, S.E. (2001) Neurodegenerative disease: the neuronal ceroid lipofuscinoses (Batten disease). *Curr. Opin. Neurol.*, **14**, 795–803.

8. Siintola, E., Lehesjoki, A.E. and Mole, S.E. (2006) Molecular genetics of the NCLs—status and perspectives. *Biochim. Biophys. Acta*, **1762**, 857–864.
9. Vesa, J., Hellsten, E., Verkruyse, L.A., Camp, L.A., Rapola, J., Santavuori, P., Hofmann, S.L. and Peltonen, L. (1995) Mutations in the palmitoyl protein thioesterase gene causing infantile neuronal ceroid lipofuscinosis. *Nature*, **376**, 584–587.
10. Zhang, Z., Lee, Y.C., Kim, S.J., Choi, M.S., Tsai, P.C., Xu, Y., Xiao, Y.J., Zhang, P., Heffer, A. and Mukherjee, A.B. (2006) Palmitoyl-protein thioesterase-1 deficiency mediates the activation of the unfolded protein response and neuronal apoptosis in INCL. *Hum. Mol. Genet.*, **15**, 337–346.
11. Wei, H., Kim, S.J., Zhang, Z., Tsai, P.C., Wisniewski, K.E. and Mukherjee, A.B. (2008) ER- and oxidative-stresses are common mediators of apoptosis in both neurodegenerative and non-neurodegenerative lysosomal storage disorders and are alleviated by chemical chaperones. *Hum. Mol. Genet.*, **17**, 469–477.
12. Zhang, Z., Lee, Y.C., Kim, S.J., Choi, M.S., Tsai, P.C., Saha, A., Wei, H., Xu, Y., Xiao, Y.J., Zhang, P. *et al.* (2007) Production of lysophosphatidylcholine by cPLA2 in the brain of mice lacking PPT1 is a signal for phagocyte infiltration. *Hum. Mol. Genet.*, **16**, 837–847.
13. Saha, A., Kim, S.J., Zhang, Z., Lee, Y.C., Sarkar, C., Tsai, P.C. and Mukherjee, A.B. (2008) RAGE signaling contributes to neuroinflammation in infantile neuronal ceroid lipofuscinosis. *FEBS Lett.*, **582**, 3823–3831.
14. Gupta, P., Soyombo, A.A., Atashband, A., Wisniewski, K.E., Shelton, J.M., Richardson, J.A., Hammer, R.E. and Hofmann, S.L. (2001) Disruption of PPT1 and PPT2 causes neuronal ceroid lipofuscinosis in knockout mice. *Proc. Natl Acad. Sci. USA*, **98**, 13566–13571.
15. Bible, E., Gupta, P., Hofmann, S.L. and Cooper, J.D. (2004) Regional and cellular neuropathology in the palmitoyl protein thioesterase-1 null mutant mouse model of infantile neuronal ceroid lipofuscinosis. *Neurobiol. Dis.*, **16**, 346–359.
16. Kim, S.J., Zhang, Z., Lee, Y.C. and Mukherjee, A.B. (2006) Palmitoyl-protein thioesterase-1 deficiency leads to the activation of caspase-9 and contributes to rapid neurodegeneration in INCL. *Hum. Mol. Genet.*, **15**, 1580–1586.
17. Knott, A.B., Perkins, G., Schwarzenbacher, R. and Bossy-Wetzel, E. (2008) Mitochondrial fragmentation in neurodegeneration. *Nat. Rev. Neurosci.*, **9**, 505–518.
18. Schon, E.A. and Manfredi, G. (2003) Neuronal degeneration and mitochonfrial dysfunction. *J. Clin. Invest.*, **111**, 303–312.
19. Puigserver, P., Wu, Z., Park, C.W., Graves, R., Wright, M. and Spiegelman, B.M. (1998) A cold inducible coactivator of nuclear receptors linked to adaptive thermogenesis. *Cell*, **92**, 829–839.
20. Miao, N., Levin, S.W., Baker, E.H., Caruso, R.C., Zhang, Z., Gropman, A., Koziol, D., Wesley, R., Mukherjee, A.B. and Quezado, Z.M. (2009) Children with infantile neuronal ceroid lipofuscinosis have an increased risk of hypothermia and bradycardia during anesthesia. *Anesth Analg*, **109**, 372–378.
21. Lin, J., Wu, P.H., Tarr, P.T., Lindenberg, K.S., St-Pierre, J., Zhang, C.Y., Mootha, V.K., Jäger, S., Vianna, C.R., Reznick, R.M. *et al.* (2004) Defects in adaptive energy metabolism with CNS-linked hyperactivity in PGC-1α-null mice. *Cell*, **119**, 121–135.
22. Carling, D. (2004) The AMP-activated protein kinase cascade—a unifying system for energy control. *Trends Biochem. Sci.*, **29**, 18–24.
23. Hardie, D.G. (2007) AMP-activated/SNF1 protein kinases: conserved energy. *Nat. Rev. Mol. Cell. Biol.*, **8**, 774–785.
24. Zong, H., Ren, J.M., Young, L.H., Pypaert, M., Mu, J., Birnbaum, M.J. and Shulman, G.I. (2002) AMP kinase is required for mitochondrial biogenesis in skeletal muscle in response to chronic energy deprivation. *Proc. Natl Acad. Sci. USA*, **99**, 15983–15987.
25. Cantó, C. and Auwerx, J. (2009) Caloric restriction, SIRT1 and longevity. *Trends Endocrinol. Metab.*, **20**, 325–331.
26. Suwa, M., Nakano, H., Higaki, Y., Nakamura, T., Katsuta, S. and Kumagai, S. (2003) Increased wheel-running activity in the genetically skeletal muscle fast-twich fiber dominant rats. *J. Appl. Physiol.*, **94**, 185–192.
27. Finkel, T., Deng, C.-X. and Mostoslavsky, R. (2009) Recent progress in the biology and physiology of sirtuins. *Nature*, **460**, 587–591.
28. Cantó, C., Gerhart-Hines, Z., Feige, J.N., Lagouge, M., Noriega, L., Milne, J.C., Elliott, P.J., Puigserver, P. and Auwerx, J. (2009) AMPK regulates energy expenditure by modulating NAD(+) metabolism and SIRT1 activity. *Nature*, **458**, 1056–1060.
29. Spiegelman, B.M. (2007) Translational control of mitochondrial energy metabolism through PGC1 coactivators. *Novartis Found. Symp.*, **287**, 60–63.
30. Pallàs, M., Casadesús, G., Smith, M.A., Coto-Montes, A., Pelegri, C., Vilaplana, J. and Camins, A. (2009) Resveratrol and neurodegenerative diseases: activation of SIRT1 as the potential pathway towards neuroprotection. *Curr. Neurovasc Res.*, **6**, 70–81.
31. Milne, J.C., Lambert, P.D., Schenk, S., Carney, D.P., Smith, J.J., Gagne, D.J., Jin, L., Boss, O., Perni, R.B., Vu, C.B. *et al.* (2007) Small molecule activators of SIRT1 as therapeutics for the treatment of type 2 diabetes. *Nature*, **450**, 712–716.
32. Li, Y., Xu, W., McBurney, M.W. and Longo, V.D. (2008) SirT1 inhibition reduces IGF-I/IRS-2/Ras/ERK1/2 signaling and protects neurons. *Cell Metab.*, **8**, 38–48.
33. Michan, S. and Sinclair, D. (2007) Sirtuins in mammals: insights into their biological function. *Biochem. J.*, **404**, 1–13.
34. Feige, J.N., Lagouge, M., Canto, C., Strehle, A., Houten, S.M., Milne, J.C., Lambert, P.D., Mataki, C., Elliott, P.J. and Auwerx, J. (2008) Specific SIRT1 activation mimics low energy levels and protects against diet-induced metabolic disorders by enhancing fat oxidation. *Cell Metab.*, **8**, 347–358.
35. Sakoda, H., Ogihara, T., Anai, M., Fujishiro, M., Ono, H., Onishi, Y., Katagiri, H., Abe, M., Fukushima, Y., Shojima, N. *et al.* (2002) Activation of AMPK is essential for AICAR-induced glucose uptake by skeletal muscle but not adipocytes. *Am. J. Physiol. Endocrinol.*, **282**, E1239–E1244.
36. Kobayashi, Y., Furukawa-Hibi, Y., Chen, C., Horio, Y., Isobe, K., Ikeda, K. and Motoyama, N. (2005) SIRT1 is critical regulator of FOXO-mediated transcription in response to oxidative stress. *Int. J. Mol. Med.*, **16**, 237–243.
37. Sedding, D.G. (2008) FOXO transcription factors in oxidative stress response and ageing—a new fork on the way to longevity? *Biol. Chem.*, **389**, 279–283.
38. Rodgers, J.T., Lerin, C., Haas, W., Gygi, S.P., Spiegelman, B.M. and Puigserver, P. (2005) Nutrient control of glucose homeostasis through a complex of PGC-1alpha and SIRT1. *Nature*, **434**, 113–118.
39. Hock, M.B. and Kralli, A. (2009) Transcriptional control of mitochondrial biogenesis and function. *Ann. Rev. Physiol.*, **71**, 177–203.
40. Wareski, P., Vaarmann, A., Choubey, V., Safiulina, D., Liiv, J., Kuum, M. and Kaasik, A. (2009) PGC-1a and PGC-1b regulate mitochondrial density in neurons. *J. Biol. Chem.*, **284**, 21379–21385.
41. Baur, J.A., Pearson, K.J., Price, N.L., Jamieson, H.A., Lerin, C., Kalra, A., Prabhu, V.V., Allard, J.S., Lopez-Lluch, G., Lewis, K. *et al.* (2006) RSV improves health and survival of mice on a high-calorie diet. *Nature*, **444**, 337–342.
42. Pearson, K.J., Baur, J.A., Lewis, K.N., Peshkin, L., Price, N.L., Labinskyy, N., Swindell, W.R., Kamara, D., Minor, R.K., Perez, E. *et al.*, (2008) Resveratrol delays age-related deterioration and mimics transcriptional aspects of dietary restriction without extending life span. *Cell Metab.*, **8**, 157–168.
43. Selman, C., Tullet, J.M., Wieser, D., Irvine, E., Lingard, S.J., Choudhury, A.I., Claret, M., Al-Qassab, H., Carmignac, D., Ramadani, F. *et al.* (2009) Ribosomal protein S6Kinase 1 signaling regulates mammalian life span. *Science*, **326**, 140–144.
44. Woloszynek, J.C., Coleman, T., Semenkovich, C.F. and Sands, M.S. (2007) Lysosomal dysfunction results in altered energy balance. *J. Biol. Chem.*, **282**, 35765–35771.
45. Stanfel, M.N., Shamieh, L.S., Kaeberlein, M. and Kennedy, B.K. (2009) The TOR pathway comes of age. *Biochim. Biophys. Acta*, **1790**, 1067–1074.
46. Valenzano, D.R., Terzibasi, E., Genade, T., Cattaneo, A., Domenici, L. and Cellerino, A. (2006) Resveratrol prolongs lifespan and retards the onset of age-related markers in short-lived vertebrates. *Curr. Biol.*, **16**, 296–300.